Faraday Discuss., 1997, **106**, 205–217

First principles calculations on crystalline and liquid iron at Earth's core conditions

Lidunka Vočadlo,[a] Gilles A. de Wijs,[b] Georg Kresse,[b,c] Mike Gillan[b] and Geoffrey D. Price[a]

[a] *Research School of Geological and Geophysical Sciences, Birkbeck College and University College London, Gower Street, London, UK WC1E 6BT*
[b] *Physics Department, Keele University, Keele, Staffordshire, UK ST5 5BG*
[c] *Institute for Theoretical Physics, Technical University of Vienna, Wiedner Hauptstrasse 8-10/136, A-1040 Vienna, Austria*

Ab initio electronic structure calculations, based upon density functional theory within the generalised gradient approximation using ultrasoft non-norm-conserving Vanderbilt pseudopotentials, have been used to predict the structure and properties of crystalline and liquid iron and solid FeSi at conditions found in the Earth's core. The quality of the pseudopotentials used was assessed by calculating well documented properties of the solid phase: we have accurately modelled the equation of state of bcc and hcp Fe and FeSi, the bcc → hcp phase transition, the magnetic moment of bcc Fe, the elastic constants of bcc Fe, the bcc → bct distortive phase transition and the phonon frequencies for fcc Fe; the results show good agreement with both theory and experiment. Simulations were also performed on liquid iron and we present the first *ab initio* quantum molecular dynamics calculations on the structure and transport properties of liquid iron under core conditions. Our calculations show that the structure of liquid iron at the conditions to be found in the outer core is highly compressed with a first-neighbour coordination number inferred from the radial distribution function of *ca.* 12. We have also predicted a diffusion coefficient of 0.5×10^{-4} cm^2 s^{-1} indicative of a core viscosity of *ca.* 0.026 Pa s, in line with current estimates.

The physical properties of iron and its alloys are of considerable interest to both material scientists and geophysicists. Geologically, the properties of solid and liquid iron are fundamental to our understanding of the behaviour of the Earth's core, including the generation of the dynamo causing the Earth's magnetic field and the structure of the solid phase in the inner core. The physical properties of solid and liquid iron at these conditions are poorly understood; this is because direct observation of the properties and structure of solid and liquid iron and its alloys is very difficult at the extreme conditions that exist at the Earth's centre, and the considerable pressure and temperatures involved prohibit definitive experimentation.

Computer simulations can provide an accurate means of calculating the thermoelastic properties of materials at high pressures (P) and temperatures (T) *via* a variety of techniques. Unfortunately, when using many of the computational methods it is often necessary to adopt a number of approximations because of computational limitations. More recently, the growing capacity of high-performance supercomputers has enabled large calculations on increasingly complex materials to be attempted; consequently the study of the full *ab initio* electronic structure of such phases has now become possible.

However, current CPU limitations still make such calculations highly time consuming and expensive. An alternative approach to all-electron calculations is the use of pseudopotentials, where approximations are made to describe the potential associated with the core electrons, and the electron density of only the valence electrons is explicitly calculated; this results in a significant reduction in the CPU requirements, thereby making the calculations more efficient.

This approach is only effective if the pseudopotentials used are able to describe the electronic and energetic state of the materials as accurately as the all-electron calculations. In our study of core phases, it is therefore essential to perform test calculations on iron phases with well documented characteristics before embarking on the technically more advanced liquid iron simulations.

In this paper we shall first review the current status of the experimentally determined iron phase diagram and the complementary computer simulations which have been carried out on this system. We then describe the methodology used in our pseudopotential calculations, and assess the quality of the pseudopotential by calculating some of the static properties of body-centred cubic (bcc), body-centred tetragonal (bct), face-centred cubic (fcc) and hexagonal-close packed (hcp) iron, and FeSi using Vanderbilt non-norm-conserving pseudopotentials within the generalised gradient approximation (GGA). We compare these results with both experiment and theoretical calculations. For these preliminary calculations we then apply this methodology to pure liquid iron, recognising that the outer core is not pure iron but has *ca.* 10% lighter alloying elements. We present the results from the first ever quantum mechanical molecular dynamics simulation of this phase at two high-P,T states representative of the boundaries of the Earth's outer core with the inner core (ICB) and the lower mantle (CMB). Finally, we discuss the geophysical significance of our initial calculations.

Review of past work

Experimental data

The status of our knowledge of the phase diagram of solid iron up to 1993 has been summarised by Anderson[1] and is shown in Fig. 1. Up to *ca.* 20 GPa and 2000 K the phase diagram is universally accepted. However, Anderson[1] has highlighted some of the areas of uncertainty associated with the high-P,T regions of the iron phase diagram where the exact structure is uncertain. Recent studies[2,3] have shown a new phase, β, which is suggested to exist near 90 GPa and *ca.* 2000 K, and another phase, Θ, inferred to exist above 200 GPa and *ca.* 4000 K. Experiments suggest that the β phase may have the dhcp (double hexagonal close-packed) structure,[2] and the Θ phase might be a high-T,P bcc phase;[4] the latter is supported by molecular dynamics calculations,[5] but is in apparent conflict with *ab initio* studies which suggest that a bct phase may be favoured.[6] Therefore, to date, there is much uncertainty as to the exact phase stability and structure of high-P,T iron.

The equation of state of liquid iron has been recently summarised by Anderson and Ahrens.[7] From a thermodynamic analysis of available ultrasonic, pulse heating and shockwave compressional data, they provide a self-consistent dataset to 10 Mbar. From this, they calculate thermodynamic properties (ρ, K, V) of pure liquid Fe along isentropes associated with the ICB temperatures of 5000, 6000, 7000 and 8000 K. The viscosity of the Earth's liquid outer core is probably close to that of pure iron at ambient pressure and has been discussed by Poirier,[8] who has analysed the transport properties of liquid metals and suggests, on the basis of empirical systematics, that the viscosity in this region takes a value of *ca.* 0.06 Pa s.

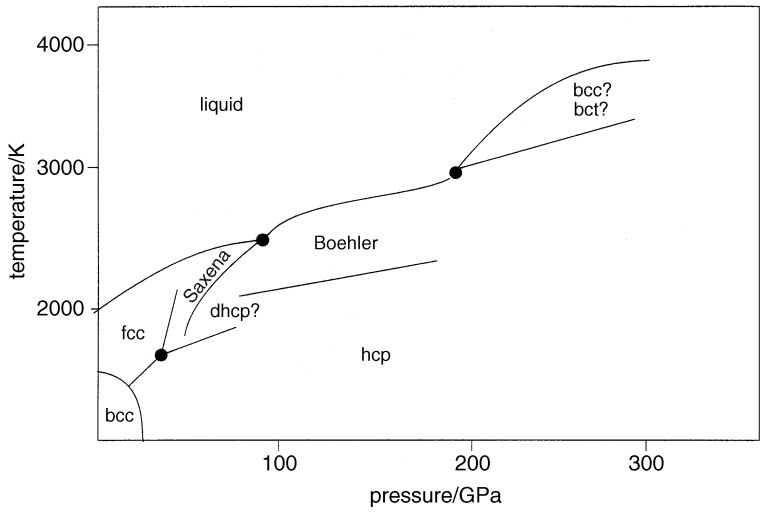

Fig. 1 Current understanding of the high-pressure phase diagram of iron; the well established low-pressure bcc, fcc and hcp phases and the unconfirmed possible dhcp and bcc–bct high-temperature phases

Simulations

Despite recent experimental progress in determining the existence of uncharacterised high-P,T phases of iron, the exact nature of their structure is still unknown. However, we can further our understanding of the structural and thermoelastic properties of solid iron phases through computer modelling. Using simulation techniques, such as pair potentials, all-electron calculations and tight-binding methods, it is possible to obtain the equation of state (EOS) as a function of pressure and temperature in an attempt to constrain the possible candidates for these high-P,T phases.

If a suitable pair-potential can be found, then a study of the high-P,T behaviour of Fe would be relatively straightforward. Matsui[5] used a potential model first described by Ross *et al.*[9] to model the EOS of the hcp and bcc phases. This simulation reproduced the EOS of hcp Fe very well; however, the problem with this type of study is that the transferability of the model potential used to different polymorphs of iron has not yet been proven. Therefore this work suffers, as do other calculations based upon empirical potentials, from the lack of reliability that can be placed on using potentials beyond the range of empirical fitting and, therefore, the confidence with which one can predict properties outside the experimental range. As a result, *ab initio* methods must be adopted.

Some of the first *ab initio* full linear augmented plane wave (FLAPW) calculations on iron were carried out by Jansen *et al.*[10,11] They concluded that their results depended critically upon the nature of the non-local corrections to the exchange and correlation, *i.e.*, use of the local density approximation (LDA) and local spin density approximation (LSDA) were insufficient to describe the electron density and hence structure and magnetic properties of iron. A significant improvement in this area was reported by Stixrude *et al.*[12] where they showed that, by using the GGA[13] in the LAPW calculations, they obtained excellent agreement with measured EOS of bcc and hcp Fe to >350 GPa. In addition, they reproduced the bcc–hcp phase transition and the bcc magnetic moment. This work was later elaborated upon by Stixrude and Cohen[6] who also reported the behaviour of fcc Fe and showed that the bcc structure becomes mechanically unstable

with respect to tetragonal strain at 150 GPa undergoing a distortive phase transition from bcc → bct.

Thus far, iron had been studied using all-electron calculations, which are intrinsically CPU intensive. To study energy–geometry space more effectively, a more approximate wavefunction is desirable. Hence, in 1995, Sasaki *et al.*[14] reported the use of pseudopotential calculations combined with LSDA for bcc iron and fcc nickel. They showed that these calculations reproduced structural and magnetic properties, as well as the all-electron calculations within the LSDA. However, although these calculations showed how the pseudopotential method could give results comparable with FLAPW, they confirmed the view, mentioned earlier,[11] that the use of the LSDA in these calculations does not give results in agreement with observation and GGA calculations.

More recently, the high-pressure phases of iron have been investigated by Söderlind *et al.*[15] using full-potential linear muffin tin orbitals (FP-LMTO) within the GGA. They confirmed previous theoretical calculations and obtained the magnetic states and EOS of the bcc, fcc, bct, hcp and dhcp polymorphs. They predict a bcc–hcp transition at 10 GPa, a metastable dhcp phase which might be accessible at high T up to 50 GPa, and confirm the mechanical instability of bcc above 100 GPa. They then went on to predict the elastic constants and phonon frequencies of fcc and hcp iron, using *ab initio* calculations within the LDA, at three volumes for both high (400 GPa) and low pressures. In addition, they fitted a many-body interaction potential to their *ab initio* calculations and used that to calculate the phonon spectra of fcc and hcp Fe.

To date, no *ab initio* studies of liquid iron have been reported, although *ab initio* studies of liquid metals in general are now becoming possible using Car–Parrinello methods.[16] The use of ultrasoft pseudopotentials has great advantages in modelling the dynamics of transition metals as shown by Pasquarello *et al.*[17] and Kresse and Hafner.[18] In the following section we outline the methodology adopted in our study of solid and liquid iron.

Calculation methodology and pseudopotentials

The simulations presented here have been carried out using first-principles density functional theory. The valence orbitals were expanded in a basis of plane waves, and the interaction between the core and the valence electrons was described by means of pseudopotentials.

Until recently most pseudopotentials have been norm-conserving.[19] The pseudopotential concept requires that the scattering properties of the pseudo-atom and of the exact atom are the same at a specified matching radius, R_{match}. Inside the matching radius the pseudo-wavefunctions are nodeless and only approximate. The matching radius controls the overall accuracy and 'transferability' of the pseudopotential. It was shown by Hamann *et al.*[19] that a good description of the scattering properties requires that the pseudo-wavefunction ϕ_{lm}^{PP} fulfils a norm-conservation condition:

$$\int_0^{R_{\mathrm{match}}} (|\,\phi_{lm}^{\mathrm{exact}}(\boldsymbol{r})\,|^2 - |\,\phi_{lm}^{\mathrm{PP}}(\boldsymbol{r})\,|^2)\,\mathrm{d}^3\boldsymbol{r} = 0 \qquad (1)$$

where $\phi_{lm}^{\mathrm{exact}}$ is the exact all-electron wavefunction, and l,m are the angular momentum quantum numbers. This restriction poses a serious problem, especially for first row transition metals, because it forces the pseudo-wavefunction to vary rapidly. The only compromise one can make is to increase the matching radius, which makes the pseudo-wavefunction 'softer' (*i.e.*, a smaller basis set might be used), but this always decreases the quality of the pseudopotential. In general, the minimum basis set size for transition metals is around 500 plane waves per atom, making calculations very expensive.

A solution to this problem was proposed by Vanderbilt[20] who showed that it is possible to give up the norm-conservation condition if one corrects for the resulting difference between the exact and the pseudo-charge density [*i.e.*, the terms between the brackets of eqn. (1)].This is achieved using localised augmentation functions centred on each atom. Giving up the norm-conservation constraint results in significantly smoother pseudo-wavefunctions. The new ultrasoft pseudopotentials give results which are very close to, or even indistinguishable from, results obtained with the best all-electron first principles methods currently available. Details of the construction of our pseudopotentials can be found in Kresse and Hafner[21] and specific information about Fe pseudopotentials from Moroni *et al.*[22]

Another point which requires some care is the description of the exchange-correlation energy. As discussed above, it is now well known that GGA must be used in order to get an accurate description of the ground-state properties of Fe at ambient pressure.[23] It has also been shown that the neglect of GGA strongly affects results at high pressure.[15] Here we have used a GGA based on the LDA of Ceperley and Alder[24] and the gradient corrections according to Perdew *et al.*[13] All the pseudopotentials have been constructed with non-linear partial core corrections.[25]

Another advantage of ultrasoft pseudopotentials is that it is possible, at least in principle, to describe lower lying 'pseudo-core' states as valence states. In the case of Fe, treating 3p states as valence turned out to be vital to get an accurate description of the pressure at conditions found in the Earth's core. However, the description of the highly localised 3p states as valence states is relatively expensive and such a description is therefore unsuitable for the more time consuming calculations on the liquid. This problem can be overcome since the effect of the 3p states can be described by a pairwise additive repulsive potential (similar to the approach Ballone and Galli[26]). Therefore, to decrease the computational costs of the liquid state simulations, we have decided to keep the 3p states in the core and to describe their effect with this repulsive pair potential.

The pseudopotential calculations presented below have been done with VASP (Vienna *ab initio* simulation package). In VASP the ground state is calculated exactly for each set of ionic positions using an efficient iterative matrix diagonalisation scheme and a Pulay mixer.[27] A smearing method was used to avoid problems with level crossing, and the electronic free energy was taken as variational quantity. More details concerning the computational method can be found in Kresse and Furthmüller.[28,29]

The results for the solid Fe/FeSi calculations described in the following section were obtained using the GGA pseudopotential with the 3p electrons treated explicitly as valence electrons, *i.e.*, with an [Ne]$3s^2$ core. The liquid calculations employed the pseudopotential with [Ar] core together with the pair potential correction. The pseudopotentials are labelled according to their frozen core configuration, *i.e.*, [Ne]$3s^2$ and [Ar].

Results

Solid iron and FeSi

To confirm fully the validity of the [Ne]$3s^2$ pseudopotential, calculations were performed on the bcc, hcp, fcc and bct structures of iron, and also on FeSi. Energy convergence as a function of k-point sampling was investigated, and all calculations reported converged to 0.01 eV in total energy per atom; as a result the calculations were performed with wavefunctions being sampled at 35 k-points in the irreducible Brillouin zone for bcc Fe and bct Fe, and 36 for hcp Fe, 344–567 for the fcc Fe phonon calculations and 11 for FeSi.

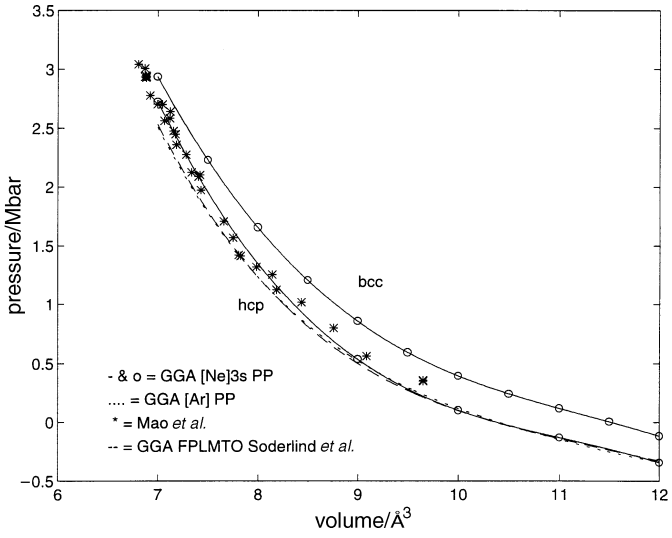

Fig. 2 Calculated pressure–volume curve at $T = 0$ K for bcc Fe and hcp Fe. The bcc Fe was simulated with the [Ne]3s^2 pseudopotential; the hcp Fe with both the [Ne]3s^2 and the [Ar] pseudopotentials. The hcp is compared with theory[15] and experiment.[30]

Fig. 2 shows the equation of state for both bcc and hcp Fe using both the [Ar] and the [Ne]3s^2 pseudopotential. The optimal c/a ratio for hcp Fe was found to be to 1.575 over a range of volumes between 14 and 24 Å^3. The results show excellent agreement with both theory[15] and experiment,[30] thus showing that the degree of precision one can get from ultrasoft pseudopotentials is more than satisfactory. Table 1 shows the results of fitting these data to a second-order Birch–Murnaghan equation, using $K' = 4$ to enable comparison with theory and experiment. The transition pressure for bcc → hcp was obtained from the enthalpy–pressure curves of the two phases and is predicited to occur at *ca.* 10 GPa, in good agreement with the FP-LMTO calculations[15] and close to the experimental value of 10–15 GPa.

Until recently, the use of the LDA to predict the magnetic properties of the ground state of iron incorrectly destabilised bcc Fe structure in favour of fcc Fe.[12] However, incorporating the GGA into the calculations stabilises the observed bcc structure and predicts a magnetic moment, μ, for bcc Fe which is in excellent agreement with the

Table 1 Atomic volumes and incompressibilities of bcc and hcp iron, and the magnetic moment of the ferromagnetic bcc phase; comparisons with all-electron calculations and experiment

		FLAPW LSDA[a] $K' \neq 4$	FLAPW GGA[a] $K' \neq 4$	VASP LSDA[b]	VASP GGA [Ar][b]	VASP GGA [Ne]3s^2 [b]	expt.[c]
bcc	V_0/Å	10.45	11.4	10.5	11.7	11.55	11.80
	K/GPa	245	189	235	156	176	162–176
	μ/atom	2.04	2.17	2.05	2.32	2.25	2.12[d]
hcp	V_0/Å	9.6	10.2	9.6	10.3	10.4	11.2
	K/GPa	344	291	309	270	290	208

[a] Ref. 12. [b] This study. [c] Ref. 31. [d] Ref. 32.

ambient experimental value (Table 1); we also predict a suppression of the magnetic moment with pressure from 2.25 at $V = 11.55$ Å^3 to 0.9 at $V = 7$ Å^3 in very good agreement with the FP-LMTO calculations.[15]

The elastic constants for fcc and hcp iron have been calculated theoretically by Stixrude and Cohen[6] and by Söderlind *et al.*,[15] the former using a tight binding fit to *ab initio* GGA and the latter using *ab initio* LDA. In order to confirm further the validity of the *ab initio* pseudopotential GGA method with the [Ne]3s^2 core, we have obtained the elastic constants for bcc Fe. The elastic constants (Table 2) were calculated for bcc Fe *via* very small distortions (<3%) of the ideal bcc structure in order to keep within the harmonic approximation. The incompressibility, given by $K = \frac{1}{3}(c_{11} + 2c_{12})$, was calculated from a Birch–Murnaghan fit to compressional data; the c_{11}, c_{12} and c_{44} elastic constants were obtained from a second-order polynomial fit through the energy–distortion curve using the following elastic strain matrices:

for the tetragonal distortion:

$$\begin{pmatrix} 1+\delta & 0 & 0 \\ 0 & 1+\delta & 0 \\ 0 & 0 & \dfrac{1}{(1+\delta)^2} \end{pmatrix} \tag{2}$$

for the shear distortion:

$$\begin{pmatrix} 1 & \delta & 0 \\ \delta & 1 & 0 \\ 0 & 0 & \dfrac{1}{1-\delta^2} \end{pmatrix} \tag{3}$$

and the elastic constants are given by:

$$\left(\frac{\partial^2 U}{\partial \delta^2}\right)_{\text{tetr}} = 6c' = \frac{6}{2}(c_{11} - c_{12}) \tag{4}$$

$$\left(\frac{\partial^2 U}{\partial \delta^2}\right)_{\text{shear}} = 4c_{44} \tag{5}$$

where U is the energy per unit volume.

At ambient conditions, the bcc structure is the most stable; however, tetragonal distortions in this structure destabilise this idealised $c/a = 1$ structure under compression, therefore making the bct structure a possible candidate for the Earth's core. Fig. 3 shows how the c/a ratio varies as a function of compression; the ideal bcc structure is the most stable close to V_0, but as the volume is reduced, the structure undergoes a transformation through a metastable state at $V = 8.5$ Å^3 to a bct structure with a c/a

Table 2 Elastic constants of the bcc Fe phase; pseudopotential calculations and experiment

	calculations	experiment[a]	experiment[b]
K/GPa	176	173	
c_{11}/GPa	289	243	226–232
c_{12}/GPa	118	138	130–136
c_{44}/GPa	115	122	116–117

[a] Ref. 33. [b] Ref. 34.

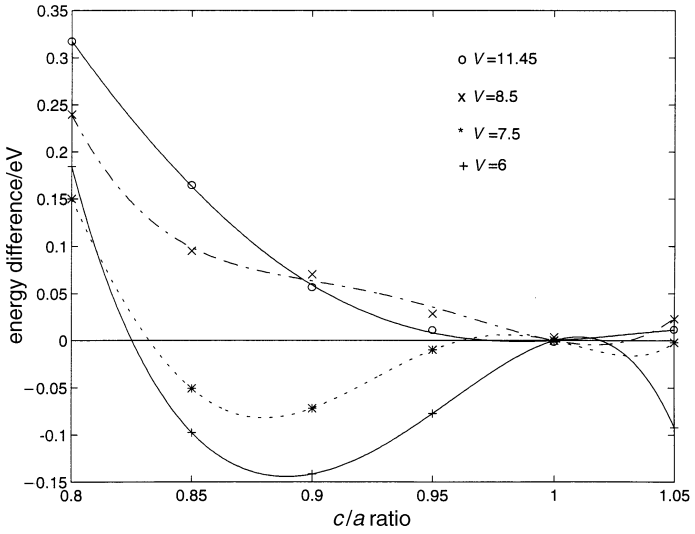

Fig. 3 Calculated energies of bct Fe as a function of compression where $c/a = 1$ is the special case of the bcc Fe structure

ratio of 0.87–0.88 at *ca.* 150 GPa, in excellent agreement with the all-electron calculations.[6,15]

To illustrate further the ability of the [Ne]$3s^2$ pseudopotential to model iron phases accurately, we have performed calculations on fcc Fe. Table 3 lists the phonon frequencies of several fcc zone-boundary phonons at a strongly compressed volume. Once more the pseudopotential is in good agreement with the FP-LMTO results.[15] Table 3 also illustrates how the pair-potential correction to the pseudopotential with the [Ar] core configuration accounts well for the change in phonon frequencies due to the compression of the 3p electrons.

Silicon is thought to be a possible alloying element in the outer core so, for our final test on core forming phases, we have performed compression calculations on FeSi. Fig. 4 shows the predicted EOS for FeSi, which is in excellent agreement with experimental data. A third-order Birch–Murnaghan fit over the full PV range gives predicted EOS parameters in good agreement with highest pressure experiments (Table 4).

Liquid iron

Having established that the pseudopotential method works extremely well for solid iron phases under compression, we now have sufficient confidence in our pseudopotentials to

Table 3 Phonon angular frequencies (10^{12} rad s^{-1}) for non-magnetic fcc Fe with volume = 6.17 $Å^3$ $atom^{-1}$

	LDA[a] FP-LMTO	LDA [Ne]$3s^2$	GGA [Ne]$3s^2$	GGA [Ar] and corr.	GGA [Ar]
L[100]	123	125	127	127	114
T[100]	85.6	84.9	88.7	86.4	78.4
L[111]	138	142	145	142	130
T[111]	60.1	59.6	60.8	59.8	55.1

[a] Ref. 15.

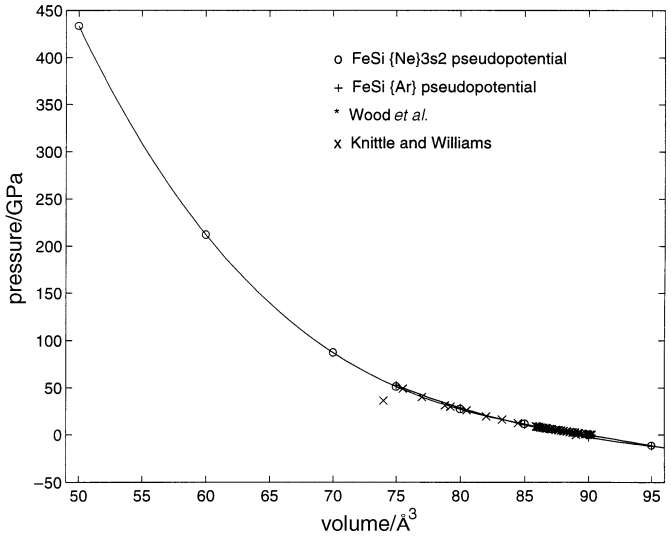

Fig. 4 Calculated pressure–volume curve for FeSi at $T = 0$ K compared with experiment[35,36]

perform simulations on liquid iron. First principles molecular dynamics simulations of non-magnetic liquid Fe were carried out at two selected thermodynamic state points representative of the ICB and the CMB. These were selected to lie on the 6000 K adiabat, which is probably representative of the temperature at the ICB[7] (see Table 5). From experimental observations and the inferred EOS of liquid Fe along the 6000 K adiabat the pressures, P_{6000} (where the subscript refers to the 6000 K adiabat) can be determined for these state points,[7] which we can compare with the pressures obtained from our simulations, P_{calc}.

We have employed a 64 atoms supercell with periodic boundary conditions, sampling wavefunctions at the Γ-point of the Brillouin zone only. The pseudopotential with an [Ar] core was used together with the pair potential correction for the additional repulsion due to compression of the 3p electrons. We used an integration time step of 1 fs and the ionic temperature was controlled with the Nosé scheme.[37] The simulations were started from a liquid sample obtained in previous simulations at ambient pressure with the positions rescaled to the required density. The ICB and CMB liquids were equilibrated for 0.7 and 1.2 ps, respectively, and statistics were gathered from 1.7 and 0.7 ps runs. The quality of the calculations was assessed by studying the total energy conservation which showed the drift corresponding to a temperature change of 40 K ps^{-1} for

Table 4 Birch–Murnaghan equation of state parameters for FeSi; pseudopotentials calculations, time-of-flight neutron diffraction[a] and X-ray diffraction experiments[b]

	Wood *et al.*[b]	Knittle and Williams[c]	PP[Ne]3s^2
V_0/Å	90.25	89.02	89.92
K/GPa	147	209	218
K'	7.7	3.5	4.2

[a] Ref. 34. [b] Ref. 35. [c] Ref. 36.

Table 5 Temperature (T) and density (ρ) at which simulations were carried out, the corresponding pressure (P_{6000}),[7] the simulated pressure (P_{calc}) and the self-diffusion coefficient (D) as obtained from the simulations of liquid Fe at the state points representative of the ICB and the CMB

	ICB	CMB
T/K	6000	4300
ρ/g cm^{-3}	13.3	10.7
P_{6000}/Mbar	3.30	1.35
P_U/Mbar	3.05	1.10
P_{pair}/Mbar	0.38	0.13
$P_{ideal\ gas}$/Mbar	0.12	0.07
P_{corr}/Mbar	0.03	0.02
P_{sim}/Mbar	3.58	1.32
$D/\times 10^{-4}$ cm^2 s^{-1}	0.4–0.5	0.5

the ICB simulations, but was less stable for the CMB simulations where the drift was *ca.* 100 K ps^{-1}.

The resulting simulated pressure was calculated as the sum of four contributions:

$$P_{calc} = P_U + P_{pair} + P_{ideal\ gas} + P_{corr} \tag{6}$$

P_U is the potential-energy contribution, which is the only term affected by k-point sampling. To check whether there might be an effect due to the limited k-point sampling we calculated the pressure for a (ICB) configuration with four k-points instead of the Γ-point only. This resulted in a change of P_U of less than 10 kbar and the electronic density of states was found to be hardly affected, therefore validating the use of our restricted sampling. P_{pair} is the contribution caused by the pair potential that mimics the correction originating from the compression of the 3p electrons. $P_{ideal\ gas}$, the kinetic contribution, is the ideal gas pressure at the temperature and density of our calculation. P_{corr} is a correction to P_U due to the incompleteness of our plane-wave basis set and it was obtained from calculations on hcp Fe, and is found to be very small (34 kbar for ICB, 23 kbar for CMB). The pressure, P_{calc} and its breakdown into various contributions are listed in Table 5. The calculated pressures agree within less than 10% with the P_{6000} values expected from the EOS of Anderson and Ahrens,[7] which gives us confidence that our simulations are capable of describing liquid Fe at Earth's core conditions.

For crystalline solids the highest coordination, 12, arises for atoms in closely packed arrangements, like hcp and fcc. In liquids, the coordination number cannot be defined completely unambigously, but a reliable number can be obtained by integration of the pair distribution, $g(r)$, to the minimum beyond the first peak. Fig. 5 shows the g values for both high-P,T simulations; integration to the first minimum yields coordination numbers of 13.8 and 13.5 for ICB and CMB, respectively, indicative of a very close-packed liquid.

In the liquid phase, atoms exhibit a diffusive behaviour which can be characterised by a self-diffusion coefficient, D. This coefficient is most easily calculated from the mean squared displacement (MSD) *via* the Einstein relation:

$$\langle |\boldsymbol{R}(t) - \boldsymbol{R}(0)|^2 \rangle = 6Dt \quad \text{for } t \to \infty$$

where $\boldsymbol{R}$ stands for an atomic position and the brackets denote a thermal average. After a sufficiently long lapse of time the MSD should increase linearly with time, allowing D

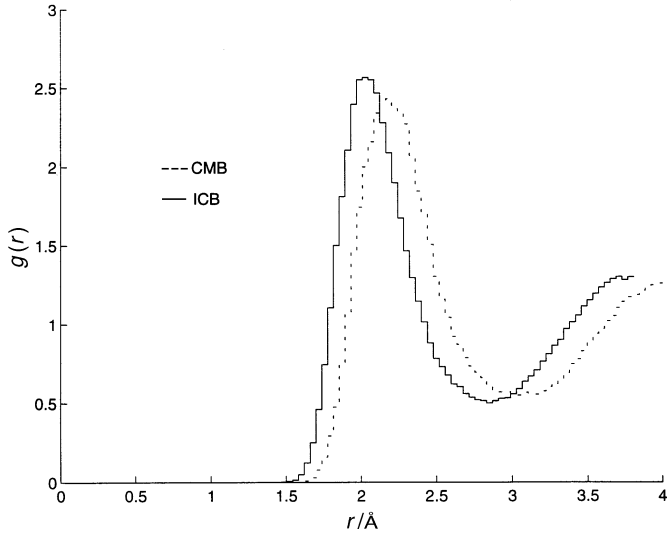

Fig. 5 Radial distribution functions obtained from simulations at the selected ICB and CMB conditions (full and dashed curves, respectively)

to be calculated. Fig. 6 shows the MSD for both the ICB and CMB runs. The diffusive behaviour and linear increase with time are obvious. The diffusion coefficients extracted are listed in Table 5 and are of the same order of magnitude as those of many liquid metals at ambient pressure. As discussed by Poirier,[8] a possible explanation for this is that, for liquid metals under compression, the activation energy for diffusion is a constant close to the melting curve and so the viscosity at high pressure might be expected to be similar to that at ambient pressure.

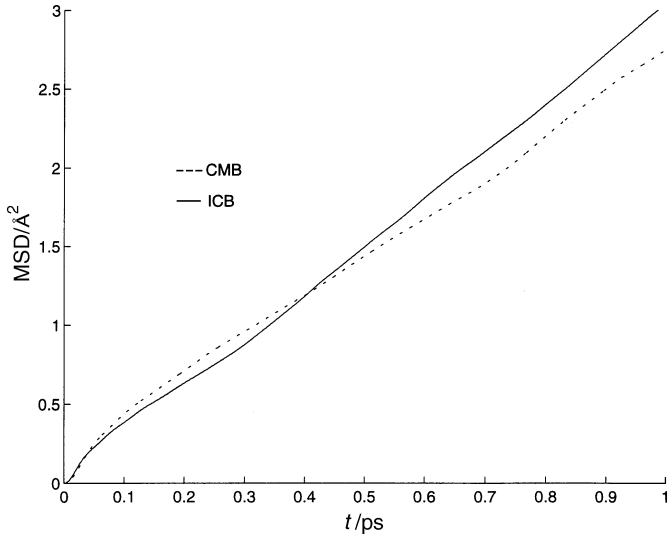

Fig. 6 Mean-squared displacements obtained from simulations at the selected ICB and CMB conditions (full and dashed curves, respectively)

Using these results we may make an estimate for the viscosity of liquid iron at core conditions *via* the Stokes–Einstein relation:

$$D\eta = \frac{k_B T}{2\pi a}$$

where D is the diffusion coefficient, η is the viscosity coefficient, k_B is Boltzmann's constant, T the temperature and a is an atomic size parameter. With $D \approx 0.4$–0.5×10^{-4} cm^2 s^{-1}, $T \approx 6000$ K and $a \approx 1$ Å, this leads to a value for the viscosity of $\eta \approx 0.026$–0.03 Pa s, which is not dissimilar to the estimates[8] based upon empirical systematics for the viscosity of the outer core of 0.06 Pa s.

Conclusions

First-principle calculations using the non-norm-conserving ultrasoft pseudopotential method within the GGA have proven to be very successful at predicting the static properties and equations of state of solid iron and FeSi. We have used this method to predict the structure and properties of liquid iron. Our calculations show that, at the conditions of the outer core, liquid iron is very close packed with a coordination number of $\geqslant 12$. First estimates of the viscosity of liquid iron under these conditions give a value of 0.16–0.2 Pa s, close to the expected value for the outer core of *ca.* 0.06 Pa s.

These are the first *ab initio* calculations on liquid iron and our preliminary investigations have led to excellent results. There is much scope for using the ultrasoft pseudopotential methodology to simulate both solid and liquid phases in the future, and to predict ultimately the full phase diagram and melting curve of iron and its alloys. We are currently focusing on simulating the high-temperature properties of crystalline iron using the frozen-phonons approach, and on performing further calculations and analysis of the melt structure of iron at core conditions.

References

1 O. L. Anderson, *AIP Conference Proceedings*, American Institute of Physics, New York, 1993.
2 S. K. Saxena, L. S. Dubrovinsky and P. Häggkvist, *Geophys. Res. Lett.*, 1996, **23**, 2441.
3 R. Boehler, *Nature* (*London*), 1993, **363**, 534.
4 W. A. Bassett and M. S. Weathers, *J. Geophys. Res.*, 1990, **95**, 21709.
5 M. Matsui, *AIP Conference Proceedings*, American Institute of Physics, New York, 1993.
6 L. Stixrude and R. E. Cohen, *Geophys. Res. Lett.*, 1995, **22**, 125.
7 W. W. Anderson and T. J. Ahrens, *J. Geophys. Res.*, 1994, **99**, 4274.
8 J. P. Poirier, *Geophys. J.*, 1988, **92**, 99.
9 M. Ross, D. A. Young and R. Grover, *J. Geophys. Res.*, 1990, **95**, 21713.
10 H. J. F. Jansen, K. B. Hathaway and A. J. Freeman, *Phys. Rev. B*, 1984, **30**, 6177.
11 H. J. F. Jansen, K. B. Hathaway and A. J. Freeman, *Phys. Rev. B*, 1985, **31**, 7603.
12 L. Stixrude, R. E. Cohen and D. J. Singh, *Phys. Rev. B*, 1994, **50**, 6442.
13 J. P. Perdew, J. A. Chervary, S. H. Voska, K. A. Jackson, M. R. Perderson, D. J. Singh and C. Fiolhais, *Phys. Rev. B*, 1992, **46**, 6671.
14 T. Sasaki, A. M. Rappe and S. G. Louie, *Phys. Rev. B*, 1995, **52**, 12760.
15 P. Söderlind, J. A. Moriarty and J. M. Wills, *Phys. Rev. B*, 1996, **53**, 14063.
16 R. Car and M. Parrinello, *Phys. Rev. Lett.*, 1985, **55**, 1471.
17 A. Pasquarello, K. Laasonen, R. Car, C. Lee and D. Vanderbilt, *Phys. Rev. Lett.*, 1992, **69**, 1982.
18 G. Kresse and J. Hafner, *Phys. Rev. B*, 1993, **48**, 13115.
19 D. R. Hamann, M. Schlüter and C. Chiang, *Phys. Rev. Lett.*, 1979, **43**, 1494; G. B. Bachelet, D. R. Hamann and M. Schlüter, *Phys. Rev. B*, 1982, **26**, 4199.
20 D. Vanderbilt, *Phys. Rev. B*, 1990, **41**, 7892.
21 G. Kresse and J. Hafner, *J. Phys.: Condens. Matter*, 1994, **6**, 8245.
22 E. Moroni, G. Kresse, J. Furthmüller and J. Jafner, *Phys. Rev. B.*, 1997, submitted.
23 D. J. Singh, W. E. Pickett and H. Krakauer, *Phys. Rev. B*, 1991, **43**, 11628.
24 D. M. Ceperley and B. J. Alder, *Phys. Rev. Lett.*, 1980, **45**, 566; we use the parametrization by J. P. Perdew and A. Zunger, *Phys. Rev. B*, 1981, **23**, 5048.

25 S. G. Louie, S. Froyen and M. L. Cohen, *Phys. Rev. B*, 1982, **26**, 1738.
26 P. Ballone and G. Galli, *Phys. Rev. B*, 1989, **40**, 8563.
27 P. Pulay, *Chem. Phys. Lett*., 1980, **73**, 393.
28 G. Kresse and J. Furthmüller, *Comput. Mater. Sci*., 1996, **6**, 15.
29 G. Kresse and J. Furthmüller, *Phys. Rev. B*, 1996, **54**, 11169.
30 H. K. Mao, Y. Wu, L. C. Chen and J. F. Shu, *J. Geophys. Res*., 1990, **95**, 21737.
31 E. Knittle, in *Mineral Physics and Crystallography: A Handbook of Physical Constants*, ed. T. J. Ahrens, American Geophysical Union, Washington, 1995, p. 131.
32 G. G. Lonzarich, *Electrons at the Fermi Surface*, ed. M. Springford, Cambridge University Press, Cambridge, 1980, p. 225.
33 G. Simmons and H. Wang, *Single Crystal Elastic Constants and Calculated Aggregate Properties: A Handbook*, MIT Press, Cambridge, MA, 1971.
34 D. G. Isaak and K. Masuda, *J. Geophys. Res*., 1995, **100**, 17689.
35 I. G. Wood, T. D. Chaplin, W. I. F. David, S. Hull, G. D. Price and J. N. Street, *J. Phys.: Condens. Matter*, 1995, **7**, L475.
36 E. Knittle and Q. Williams, *Geophys. Res. Lett*., 1995, **22**, 445.
37 S. Nosé, *J. Chem. Phys*., 1984, **81**, 511.

Paper 7/01628J; *Received* 7*th March*, 1997